Journal of African Earth Sciences 202 (2023) 104897

Contents lists available at ScienceDirect

Journal of African Earth Sciences

journal homepage: www.elsevier.com/locate/jafrearsci

Two pulses of Mesoproterozoic intra-plate magmatism in the heart of the Palaeoproterozoic Ubendian Domain of northern Malawi

Robert J. Thomas [a,*], Steven D. Boger [a,b], Thomas Fullgraf [c], Nicolas Charles [c], Benjamin le Bayon [c], Dirk Frei [d], Alexis Plunder [c], Yann Lahaye [e], Petrus Le Roux [f], Ruth Mumba [g]

[a] Council for Geoscience, Bellville, Western Cape, 7535, South Africa
[b] School of Geography, Earth and Atmospheric Sciences, The University of Melbourne, Victoria, 3010, Australia
[c] Bureau de Recherches Géologiques et Minières, Orleans, France
[d] Department of Earth Sciences, University of the Western Cape, South Africa
[e] Geological Survey of Finland, FI-02151, Espoo, Finland
[f] Department of Geological Sciences, University of Cape Town, South Africa
[g] Geological Survey Department, Zomba, Malawi

ARTICLE INFO

Handling Editor: Dr Mohamed Mohamed G Abdelsalam

Keywords:
Malawi
Mwenga suite
Mwakikome orthogneiss
Proterozoic
Irumide
Ubendian

ABSTRACT

Two Mesoproterozoic anorogenic igneous events are recorded in the Palaeoproterozoic Ubendian Domain in northern Malawi. The oldest is represented by the Mwakikome orthogneiss, a small peraluminous, sub-alkaline and ferroan syenogranite that has a U–Pb zircon emplacement age of 1411 ± 3 Ma, an initial εNd of −4.5 and a Nd T_{DM2} model age of 2.27 Ga. These data are interpreted to suggest that the Mwakikome intrusion was derived mainly from the melting of the adjacent Palaeoproterozoic country rocks during Kibaran-aged extension. The second anorogenic igneous event is defined by the more widespread Mwenga Suite, a series of small (<100 km^2) NW-SE oriented and elongated plutons that occur in a narrow belt in the north of the Ubendian Domain. Seven samples from different intrusions gave U–Pb zircon emplacement ages between ~1150 and 1110 Ma. The Mwenga Suite is comprised of rocks that are also ferroan, potassic and sub-alkaline in composition and shows a range of major element compositions from monzogranite to alkali-feldspar granite. Nd isotopic data from one sample yielded an initial εNd of −2.2 and a Nd T_{DM2} model age of 1.88 Ga, suggesting that the suite was also largely derived from melting of the Ubendian host rocks, but with some additions from an enriched mantle source. Both the Mwakikome and Mwenga rocks are characterised by high concentrations of Zr, Hf, Nb, Ta, Y and REE and high Ga/Al, imparting a within-plate, A-type, trace element signature. The rocks have no direct temporal correlatives beyond northern Malawi and SW Tanzania and appear unique to this region. They do, however, build on a theme of long-lived Mesoproterozoic (~1400–1100 Ma) intra-plate extension, basin formation, and bimodal A-type magmatism that is better established in areas of central Africa located over 500 km NW of the study area.

1. Introduction and geological setting

The NW-trending Palaeoproterozoic Ubendian Domain in northern Malawi, is subdivided into three structurally-bounded crustal subdomains termed (from north to south) the Mbozi, Ufipa and Nyika "terranes" by Daly (1988). The central, Ufipa Subdomain, is cored by a belt of sheet-like intrusive granitic orthogneisses that are aligned parallel to the regional foliation over a distance of almost 200 km (Fig. 1).

On the British Geological Survey maps and bulletins of the 1960s and 1970s these rocks were considered to be > 1800 Ma in age (Ray, 1974, 1975; Stephens and Ray, 1978; Fitches and Ray, 1980; Stephens et al., 1991). Ray (1974) presented a Rb–Sr mineral-whole rock isochron age of 1132 ± 42 Ma, obtained by combining analyses from several intrusions, which he interpreted to date the timing of Mesoproterozoic (Irumide) metamorphism superimposed on the granites. This interpretation was contradicted by Ring et al. (1999) who obtained single-grain zircon evaporation and vapour digestion crystallisation ages of ~1119 to 1087 Ma for a number of the granites (see Fig. 1). Geochemical data reported by Ring et al. (1999) further classified these rocks as A-type granites, and their subsequent deformation was interpreted to be

* Corresponding author.
E-mail address: bthomas@geoscience.org.za (R.J. Thomas).

https://doi.org/10.1016/j.jafrearsci.2023.104897
Received 17 October 2022; Received in revised form 20 February 2023; Accepted 21 February 2023
Available online 2 March 2023

Neoproterozoic (Pan-African) in age, based on Ar–Ar hornblende ages of ~550 Ma obtained from the granites and their reworked Palaeoprotrerozoic (Ubendian) wall rocks. Ring et al. (1999) additionally estimated peak Pan-African metamorphic conditions to have reached ~680–740 °C and ~12–13 kbar. This interpretation was consistent with that of Fitches (1971) who concluded that the effects of the Irumide orogeny did not extend east of the Mafingi Hills of NW Malawi, although it contradicted the findings of an earlier study by Ring (1993) who considered the fabrics in these granitoids, and those which define the Mugesse Shear Zone, to be Irumide (~1.1 Ga) in age.

The intrusions were grouped within the "Mwenga Suite" by the GEMMAP project (Thomas et al., 2022a; Le Bayon et al., 2022) and the purpose of this paper is to provide the first overview of this suite of enigmatic granitoids. We present seven new U–Pb zircon ages from Mwenga Suite intrusions, along with Sm–Nd and Rb–Sr isotope data and major and trace element geochemical analyses in order to constrain the petrological conditions of their emplacement. In the course of the zircon dating, one intrusion was found to be considerably older and data from this body – the Mwakikome orthogneiss pluton – are also presented.

2. Mwakikome orthogneiss

The Mwakikome orthogneiss crops out in the far north of Malawi close to the border with Tanzania (Fig. 1; Locality KA8350). It is a coarse-grained and leucocratic, K-feldspar megacrystic augen gneiss with minor biotite and locally contains distinctive macroscopic magnetite (Fig. 2a). At a regional scale the distribution of the Mwakikome intrusion was mapped using its high K, Th and U radiometric signature, which distinguishes it from the surrounding layered gneisses. The orthogneiss forms a single, NW-SE oriented, lens-shaped intrusion measuring ~7 km long by ~1.5 km at its widest point. It is bounded to the NE and SW by mylonites of the Pan-African Mugesse set of shear zones. The northern margin shear zone also corresponds to the tectonic boundary between the Ufipa and Mbozi subdomains. To the SE it is presumed to be intrusive into Palaeoproterozoic amphibolite gneisses of the Ufipa Group, though the contacts were nowhere observed.

3. Mwenga Suite

The Mwenga Suite comprises a number of elongate, NW-SE oriented intrusions within the Ufipa Subdomain. They are concentrated in a ~20

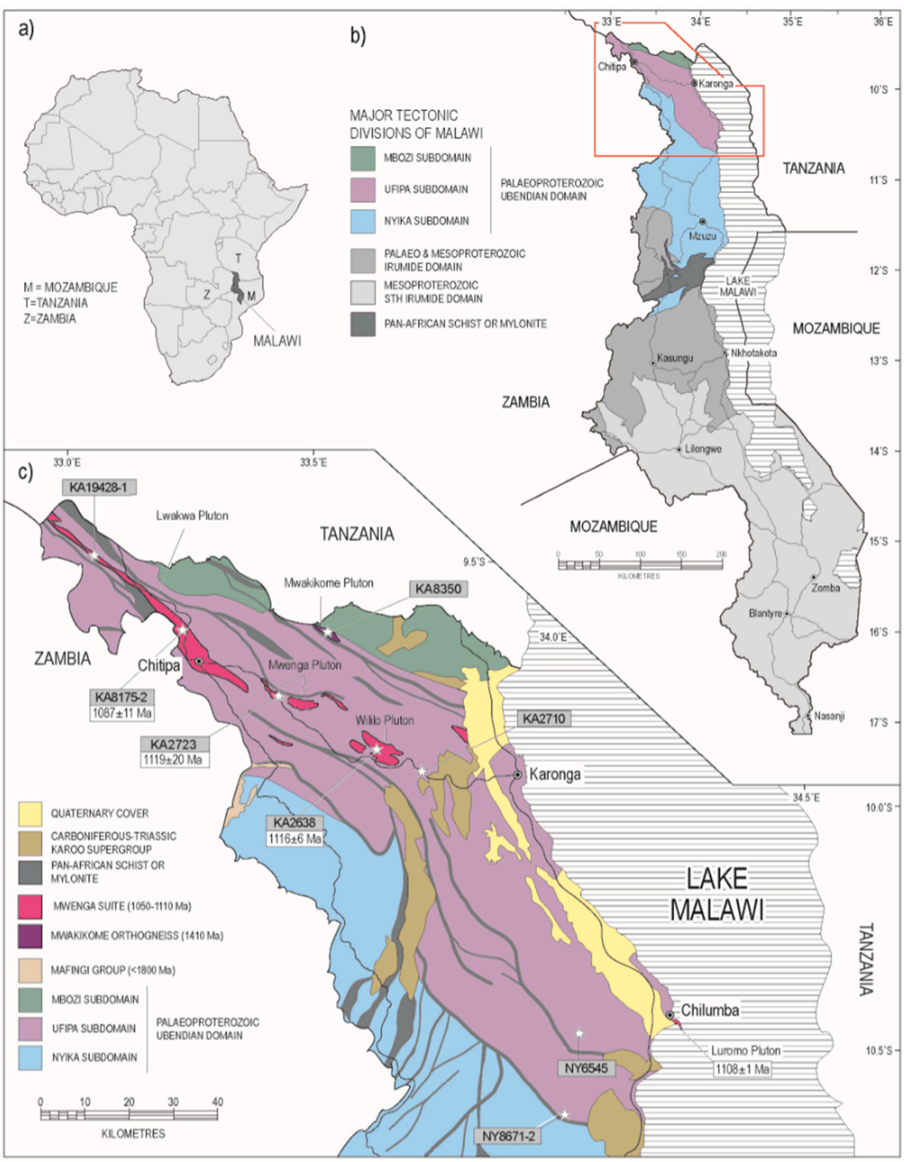

Fig. 1. Location maps. a) Malawi in south-central East Africa; b) Location of the study area in northern Malawi, with regional tectonic subdivisions, including distribution of the Palaeoproterozoic Ubendian subdomains. The area outlined in red is enlarged in c c) Simplified geological map of the study area (from Fullgraf et al., 2021) and location of the dated samples (grey boxes). White boxes are dates from Ring et al. (1999) with approximate locations. The NW trending distributed zones of Pan-African schist and mylonite that overprint the Ufipa Subdomain collectively define the Mugesse Shear Zone.

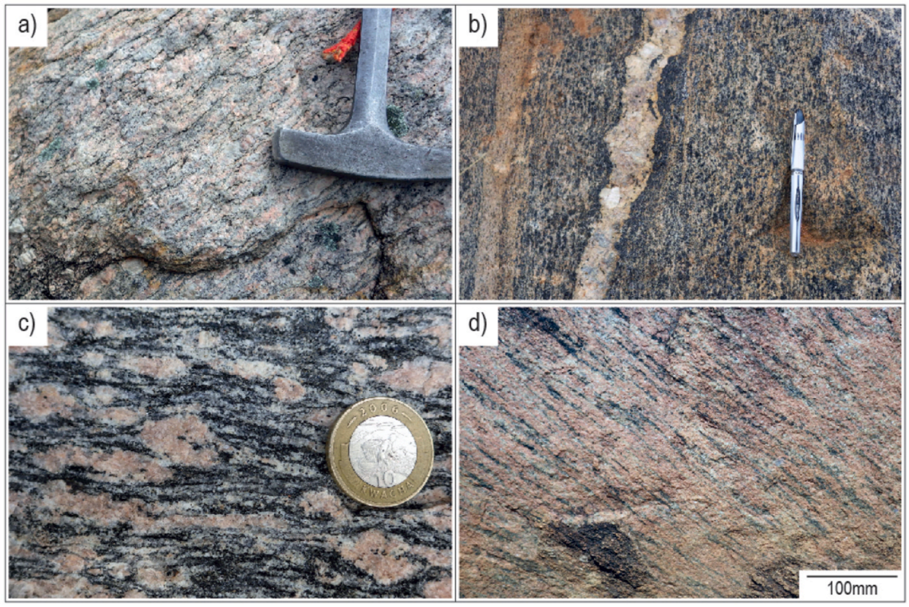

Fig. 2. Field photographs. a) Coarse-grained leucocratic Mwakikome granitic orthogneiss (Locality KA8350); b) Mwenga pluton: biotite-hornblende granitic orthogneiss from disused quarry at locality KA2723, with felsic inclusion (left) and late pegmatitic vein (left centre); c) Augen gneiss of the Lwakwa intrusion (Locality KA8175); d) Streaky pink leucogranite gneiss from the Wililo pluton (Locality KA2638).

km wide, NW-SE trending belt that can be traced from the NW tip of Malawi to south of the Luromo Peninsula, near Chilumba on Lake Malawi, a distance of almost 200 km (Fig. 1). Their distribution was mapped by both field observation and airborne magnetic and radiometric geophysical datasets. In the reduced-to-pole and total magnetic intensity datasets the signature of Mwenga Suite granitoids is varied but with generally lower magnetic susceptibility compared to that of their Ubendian country rocks. The radiometric dataset is more useful as the Mwenga Suite intrusions show generally moderate to high K, Th, and U signals that are typically higher than their country rocks(Fig. 3).

4. Analytical methods

Samples from the Mwakikome orthogneiss and Mwenga Suite were analysed for major and trace elements by Inductively Coupled Plasma Mass Spectrometry (ICP-MS) at Analytical Laboratory Services (ALS), South Africa. Three samples underwent U–Pb zircon dating by ICP-MS at the University of Nancy, France, four at the University of Stellenbosch, South Africa and one sample at the Geological Survey of Finland (GTK) laboratories in Finland. Radiogenic isotope analyses were made at the University of Cape Town, South Africa. All methods employed are

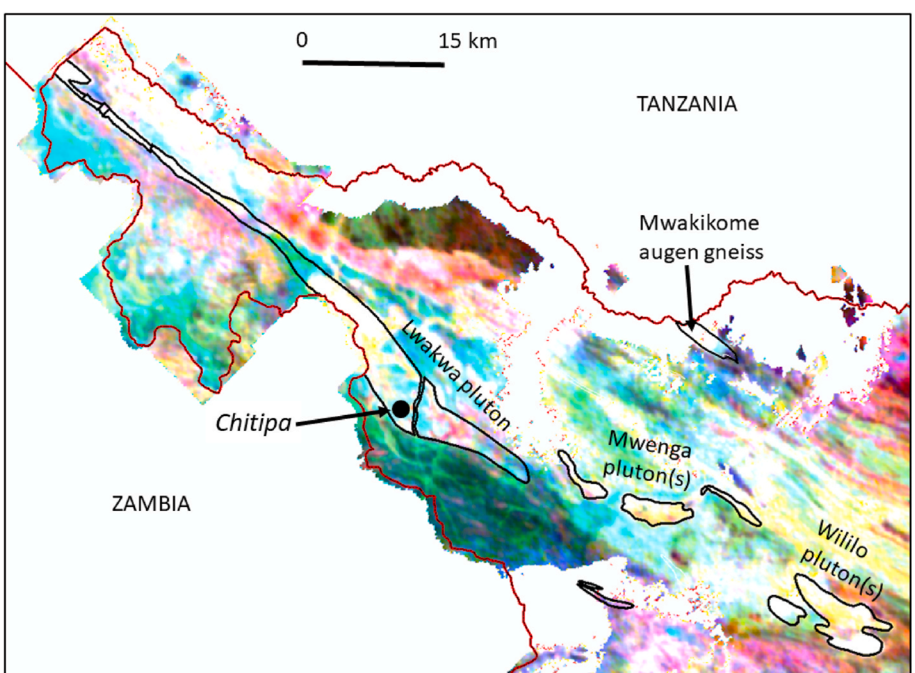

Fig. 3. Ternary K–Th–U radiometric image of NW Malawi, showing the moderate to high radioelement concentrations in the Mwenga Suite (mainly represented by white which means relatively high values of all three elements; other hues refer to higher values of one or two elements only). The radiometric data are taken from the airborne geophysical survey of Malawi conducted prior to GEMMAP.

described in supplementary Appendix 1.

5. Geochronology

Locations of the geochronological samples are shown on Fig. 1, with x-y UTM co-ordinates in Appendix 2, along with the analytical data. Sample photographs, zircon descriptions and CL images with the analytical spots are given in Appendix 3.

5.1. Mwakikome orthogneiss

Mwakikome orthogneiss sample **KA8350** was collected from far northern Malawi (Fig. 1). It is a coarse-grained, leucocratic, granitic augen orthogneiss, with recrystallised K-feldspar megacrysts up to ~2 cm in size, biotite and macroscopic magnetite. Zircons separated from this rock are mostly euhedral and elongate with cathodoluminescence (CL) images of these grains showing concentric magmatic growth zoning, consistent with high values for Th/U (0.2–1.7). Rare xenocrystic cores were observed in some grains, but none were analysed.

Forty-four analyses were carried out on zircon grains from this sample. Twenty-nine analyses scatter on, above, and below concordia (Fig. 4a) to define a discordia line that projects towards a zero age lower intercept. These data define an upper intercept age of 1417 ± 3 Ma and a statistically identical weighted mean $^{207}Pb/^{206}Pb$ age of 1411 ± 3 Ma (MSWD = 1.4). A subset of the most concordant analyses (n = 7) overlap on concordia and yield a concordia age of 1417 ± 3 Ma (Fig. 4b).

5.2. Mwenga Suite

Seven samples from various intrusions of the Mwenga Suite were collected for geochronology.

5.2.1. Mwenga Pluton

The Mwenga intrusion (Fig. 1) comprises western and eastern bodies, measuring approximately 6 x 1 and 7 × 2 km, respectively. A thin sill-like body to the NW, unexposed, but apparent in the radiometric data may be a related intrusion. The western body is comprised of a coarse-grained granitoid orthogneiss with quartz-feldspar-biotite, hornblende and rare garnet. Colour Index ranges from ~15 to 25 and there is a strong foliation and mineral lineation. While generally rather homogeneous and sub-equigranular, a weak foliation-parallel compositional layering accompanied by subtle grain-size variation is locally developed. The granite is cut by leucocratic veins and encloses elongated country rock enclaves of medium-grained, sugary garnet leucogneiss (Fig. 2b). Along its northern margin this intrusion is coarser-grained and porphyroclastic and resembles an augen gneiss. The eastern body is similar, but poorly exposed and rather more leucocratic. It is comprised of a pinkish-weathering, coarse-grained biotite granitic orthogneiss with rare amphibole.

Sample **KA2723** was collected from the western body of the Mwenga intrusion exposed in a disused quarry located approximately 20 km SE of Chitipa. The zircons from this rock are mostly subhedral to euhedral and show a broad magmatic zoning in CL imagery. Very small xenocrystic cores are also observed. Th/U is mostly between 0.4 and 0.9, although the two youngest grains with $^{207}Pb/^{206}Pb$ ages of ~1040 Ma (analyses 14 and 25) have Th/U of 0.2 or lower.

Thirty-one spot analyses were made from 23 zircon grains with the majority of data plotting on or close to concordia (Fig. 5a). The observed $^{207}Pb/^{206}Pb$ ages varied between 1173 ± 63 Ma and 1037 ± 84 Ma, with 26 analyses grouping to gave a weighted mean $^{207}Pb/^{206}Pb$ age of 1138 ± 12 Ma (MSWD = 0.2). Sixteen of the most concordant of these analyses yield an identical concordia age of 1130 ± 5 Ma (Fig. 5b). Three analyses plot away from the main grouping (Fig. 5a) and, when these two groups are combined, a poorly defined discordia line with upper and lower intercepts of 1145 ± 19 Ma and ~500 Ma can be defined. The weighted mean $^{207}Pb/^{206}Pb$ age of 1138 ± 12 Ma is taken to date the intrusion of the Mwenga granite, while the slight dispersion towards the ~500 Ma lower intercept is considered to be the result of Pb-loss during Pan-African metamorphism. Evidence for isotopic disturbance during the Pan-African event is better developed in a number of the following samples.

5.2.2. Lwakwa pluton

The Lwakwa pluton forms a narrow, NW-striking sheet-like intrusion that is ~60 km long and up to ~5 km wide. It lies NW of the Mwenga pluton (Fig. 1) within a complex zone of anastomosing mylonites that form part of the Mugesse Shear Zone. The main part of the pluton tends to be expressed topographically as a NW-SE oriented ridge with large dome-shaped fresh outcrops. The rocks are well-foliated and to a lesser extent locally compositionally banded, with amphibole- and biotite-rich ± garnet layers/aggregates alternating with quartz- and feldspar-rich layers. The central part of the intrusion is locally porphyroclastic comprising a megacrystic augen gneiss (Fig. 2c). Quartz typically forms dynamically recrystallised high-strain ribbons, although the intrusion is also locally fractured at high-angles to the ductile foliation. The intrusion is characterised by a low magnetic anomaly and a rather variable radiometric signature with the augen gneiss variant enriched in K.

Two samples from the Lwakwa pluton were taken for geochronology. Sample **KA8175–2** was collected from outcrops about 10 km NW of Chitipa in the main part of the intrusion. Zircons from this sample are relatively small, generally subhedral to euhedral in habit, although some rounded grains were also present. Aspect ratios are between 2 and 4 and CL images of these grains show fine to broad magmatic growth zoning, with xenocrystic cores present in some grains. Some grains additionally

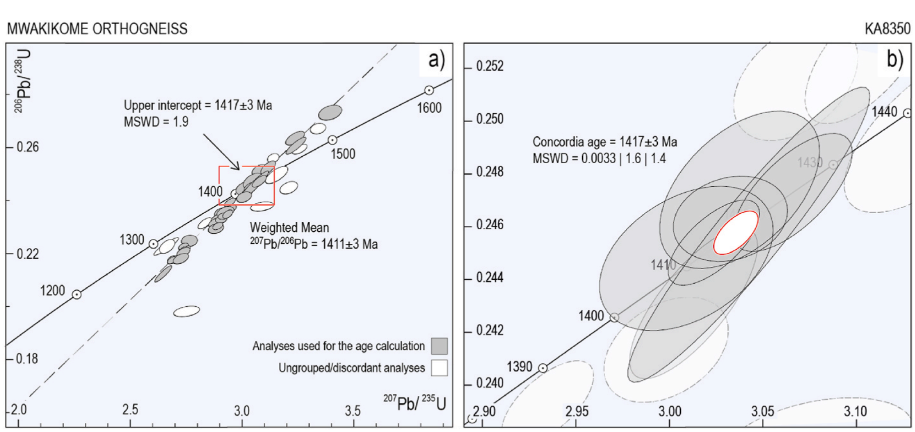

Fig. 4. Wetherill concordia plots of U–Pb zircon data from the Mwakikome orthogneiss. a) Distribution of analyses with upper intercept and weighted mean ages. Red boxed area enlarged in b). b) Subset of most concordant analyses (n = 7) used to define concordia age.

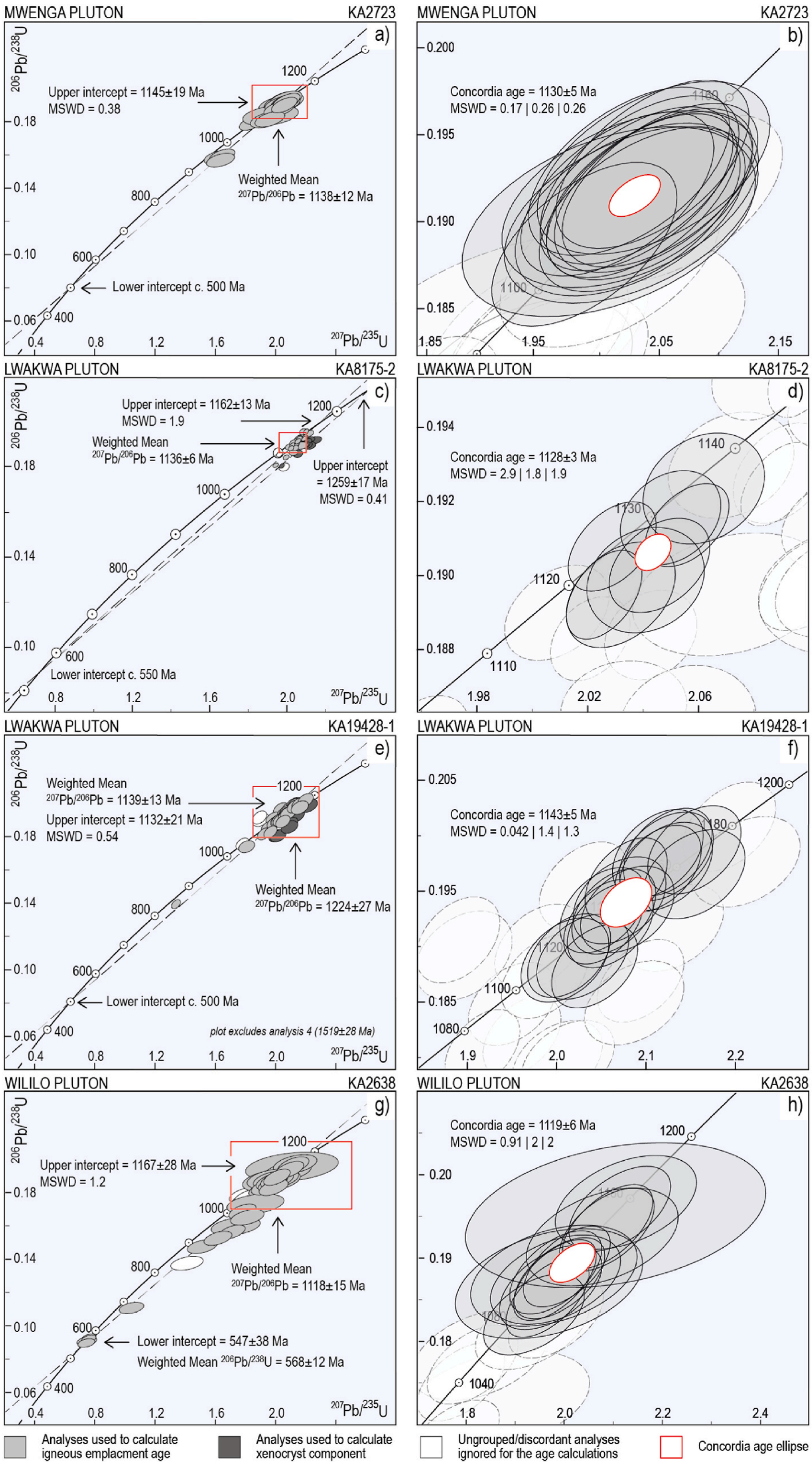

Fig. 5. Wetherill concordia plots of U–Pb zircon data for the main plutons of the Mwenga Suite. a) Mwenga Pluton, locality KA2723. Red boxed area enlarged in b). b) Subset of 16 most concordant analyses used to define concordia age. c) Lwakwa Pluton, locality KA8175. Red boxed area enlarged in d). d) Subset of 8 most concordant analyses used to define concordia age. e) Lwakwa Pluton, locality KA19428. Red boxed area enlarged in f) Subset of 18 most concordant analyses used to define concordia age. g) Wililo Pluton, locality KA2638. Red boxed area enlarged in h). Subset of 16 most concordant analyses used to define concordia age. Ages stated with 2σ confidence intervals.

show a narrow homogenous low-CL metamorphic rim that was not analysed. Th/U values for the zircons varies between 0.4 and 1.3.

Thirty-three spot analyses spots were carried out and the resulting data plot as a cloud on and somewhat below concordia with Individual $^{207}Pb/^{206}Pb$ ages scattering between ~1210 and 1100 Ma. The dataset was arbitrarily divided into two age groups based on some age clustering in the dataset, the degree of concordance, and achieving acceptable MSWD values for each group (Fig. 5c). The younger, larger, age group (light grey ellipses in Fig. 5c) comprises 22 of the more concordant analyses. These combine to give a weighted mean $^{207}Pb/^{206}Pb$ age of 1136 ± 6 (MSWD = 1.2), with a subset of 8 of the most concordant analyses further grouping to give a concordia age of 1128 ± 3 Ma (Fig. 5d). Combined with a small number of somewhat more discordant grains, these analyses distribute along a potential Pb-loss discordia that gives an upper intercept age of 1162 ± 13 Ma and a poorly-defined lower intercept around 550 Ma.

The second age group is defined by the remaining 9 analyses. These are marginally less concordant (91–95%) and yield somewhat older ages (dark grey analyses in Fig. 5c) as compared with the first group. They also show some dispersion along a discordia line and yield upper and lower intercepts ages of 1259 ± 17 Ma and ~550 Ma respectively. Given that none of the analyses within this group intersect concordia, and there is limited dispersion along the discordia line, the meaning of the upper intercept age obtained from this group remains speculative. One possibility is that this age group may date a xenocryst component within this rock, an interpretation supported by the age data obtained from the second sample from the Lwakwa pluton described below. The weighted mean $^{207}Pb/^{206}Pb$ age obtained from the largest of the two age groups measured in this rock (1136 ± 6 Ma) is taken as the best estimate for the intrusion age of the Lwakwa pluton, while the poorly defined lower intercept ages at ~550 Ma are interpreted to reflect the effects of Pan-African metamorphism.

Sample **KA19428–1** is a pinkish granitoid orthogneiss from the far NW part of the Lwakwa intrusion. The zircons obtained from this rock are subhedral to euhedral is shape and CL images display typical fine to broad magmatic growth zoning. Some crystals also show sector zoning and CL-dark inherited cores where present in some grains. Th/U values varied between 0.3 and 1.0 for the majority of grains, although Th/U was lower (<0.2) for the analysis spot that showed the most dispersion towards the lower intercept.

Thirty-seven analyses were undertaken for this rock and these yield a scatter of data points that disperse along and below the concordia curve. Individual $^{207}Pb/^{206}Pb$ ages are between ~1240 Ma and 920 Ma (Fig. 5e), with one outlier that has a $^{207}Pb/^{206}Pb$ age of ~1520 Ma. Similar to the previous sample, the dispersion of $^{207}Pb/^{206}Pb$ ages is large and two arbitrary groups based on $^{207}Pb/^{206}Pb$ age are defined. The largest of these is defined by 23 of the analyses (light grey ellipses in Fig. 5e) and together, these grains define a weighted mean $^{207}Pb/^{206}Pb$ age of 1139 ± 13 Ma (MSWD = 1.0). A subset of 18 of the most concordant analyses from this group overlap to define a concordia age of 1143 ± 5 Ma (Fig. 5f). In addition, there is some dispersion in the data from this age grouping and, when the lower intercept is fixed at ~500 Ma (a realistic age for Pan-African metamorphism), the resultant upper intercept gives an age of 1129 ± 20 Ma (MSWD = 0.56). The second age group comprises 6 analyses that yield a weighted mean $^{207}Pb/^{206}Pb$ age of 1224 ± 27 Ma. Similar to the results from the previous sample, these analyses are less concordant (87–95%) when compared to the younger dominant age grouping. The geological meaning of these analyses remains uncertain, although they may date a xenocrystic component.

5.2.3. Wililo pluton

The Wililo orthogneiss covers an area of about 35 km^2. Ray (1975) gives a detailed geological map of the intrusion, showing a plethora of small associated microgranite dykes which are found up to 13 km away from the granite. Geophysically, the granite is characterised by a somewhat variable radiometric signature. It has high K throughout, but Th and U tend to be high in the NW and SE segments only. The radiometric data clearly show a small, High-K/Th/U satellite body to the east of the main pluton, which was confirmed in outcrop. The orthogneiss forms wooded hills with rounded outcrops, sub-outcrops and loose boulders of sugary-textured, pink, very quartz- and feldspar-rich streaky, but relatively homogeneous, coarse-grained leucogranite gneiss (Fig. 2d). Mafic mineral content is very low (<5%) with biotite forming elongate flakes, small aggregates and thin schlieren, locally with magnetite and, more rarely, minute amounts of small (mm-scale) grains of pink garnet. The small satellite body in the SW is made up of similar brick-red, medium-to coarse-grained streaky leucogneiss and contains restricted zones with fibrous sillimanite. One of the minor intrusions associated with the Wililo pluton is represented by sample KA2701 which is a layer-parallel sheet within Ufipa Group gneisses, some 10 km SE of the main pluton.

Sample KA2638 was collected from outcrops of the Wililo pluton east of the main Chitipa-Karonga road, 35 km NW of Karonga. It is a pink, strongly foliated, coarse-grained equigranular and relatively homogeneous, leucogranitic orthogneiss, with a streaky texture caused by biotite schlieren and quartz ribbons. It is made up of quartz, microcline dominant over sodic plagioclase, with small amounts of biotite, hornblende and garnet. Zircons separated from this rock show typical magmatic growth zoning on CL images and have subhedral to euhedral habits. A few grains additionally show homogeneous high- and low-CL response rims. The zircons showing magmatic growth zoning have Th/U values of 0.3–0.9, for the rims, Th/U is < 0.1.

Thirty-four analyses were made on 18 zircon grains.28 analyses are within ~15% concordant and the dataset shows dispersion along a Pb-loss discordia line (Fig. 5g) that yields upper and lower intercept ages of 1167 ± 28 and 547 ± 38 Ma (MSWD = 1.1). At the upper intercept, 24 analyses group to give a weighted mean $^{207}Pb/^{206}Pb$ age of 1118 ± 15 Ma (MWSD = 0.9), while a subset of 16 of these analyses yield a concordia age of 1119 ± 6 Ma (Fig. 5h). At the lower-intercept, a cluster of 4 grains with Th/U < 0.1 give a weighted mean $^{206}Pb/^{238}U$ age of 568 ± 12 Ma (MSWD = 1.3). The weighted mean $^{207}Pb/^{206}Pb$ age of 1118 ± 15 Ma and the $^{206}Pb/^{238}U$ age of 1118 ± 15 Ma and 568 ± 12 Ma are taken to date the emplacement of the Wililo pluton and the timing of Pan-African metamorphism, respectively.

Sample **KA2701** is a coarse-grained, pinkish, inequigranular, highly foliated quartz-feldspar-biotite leucogneiss, taken from a road cutting about 21 km west of Karonga. It occurs within flaggy supracrustal gneisses of the Ufipa Group and represents one of the many small sill-like intrusions associated with the Wililo pluton (e.g. Ray, 1974). The sample is made up of quartz, microcline and subordinate plagioclase with minor biotite and garnet. The sample contains two zircon populations. The first, dominant population comprises subhedral to euhedral crystals with aspect ratios of ~2. They have a dark CL response and show magmatic growth zoning. The second population has a brighter CL response that also show magmatic growth zoning. One grain of the high-CL response population contained a low-CL response inherited core. Both CL groups show overlapping Th/U values; For the dark CL response grains Th/U = 0.3–0.8 and for the bright CL response grains Th/U = 0.2–0.9.

The zircon geochronology is more complex for this sample compared to that of the previous samples. Fifty-three analyses were undertaken of which 38 are <10% discordant. Two distinct age populations are present, which correspond to the CL groupings described above. The older and dominant population is comprised of magmatic-zoned, CL-dark grains. Thirty-seven analyses belong to this grouping and these grains yield both concordant and discordant data that produce a well-defined discordia line with an upper intercept age of 1997 ± 8 Ma and a lower intercept very close to the origin (Fig. 6a). From this age grouping subsets of 26 and 13 analyses provide weighted mean and concordia ages of 1999 ± 9 Ma (MSWD = 0.2) and 1987 ± 8 Ma, respectively (Fig. 6). The CL-bright zircon crystals comprise the second age population. Twelve analyses from this zircon type define a discordia line with an upper intercept age of 1115 ± 22 Ma and a lower intercept that passes through the origin (Fig. 6a). From this grouping, 11 analyses can be grouped to give a weighted mean $^{207}Pb/^{206}Pb$ of 1114 ± 20 Ma (MSWD = 0.1), 8 analyses group to give an identical concordia age of 1118 ± 8 Ma (Fig. 6b). An additional three grains yield concordant $^{207}Pb/^{206}Pb$ ages of 2067 ± 45, 2551 ± 45 and 2675 ± 38 Ma. The interpretation of the data is that the younger population dates the emplacement of the small leucogranite sheet, which is heavily

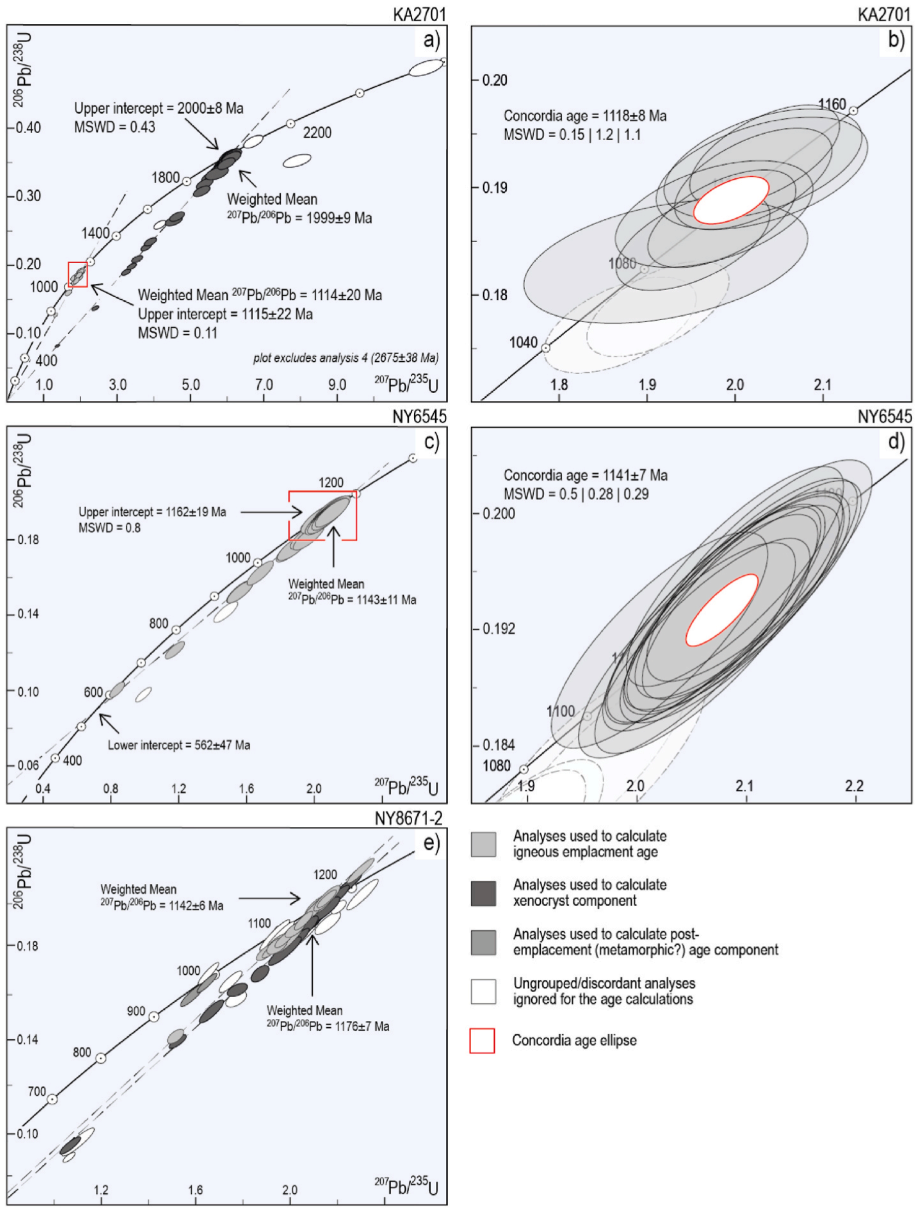

Fig. 6. Wetherill concordia plots of U–Pb zircon data from unnamed mesoscale intrusions of the Mwenga Suite. a) Locality KA2701. Red boxed area enlarged in b). b) Subset of 8 most concordant analyses used to define concordia age. c) Locality NY6545, Red boxed area enlarged in d). Subset of 14 most concordant analyses used to define concordia age. e) Locality NY8671. Ages stated with 2σ confidence intervals.

contaminated by inherited zircon grains from the host Ubendian gneisses. No evidence of later metamorphism is apparent.

5.2.4. Minor intrusions in the south Ufipa Subdomain

South of the main Mwenga Suite plutons, the Ufipa Subdomain is intruded by many small coeval leucogranitic orthogneiss bodies that are also grouped within the suite. Two samples from these bodies were dated (see Fig. 1).

Sample NY6545 is a pinkish, medium-to coarse-grained, foliation-parallel, quartz-feldspar-biotite leucogranite orthogneiss sill, from the SE Ufipa Subdomain about 21 km west of Chilumba. The zircons have subhedral grain shapes and internal magmatic growth zoning. There is some evidence for later recrystallization, while some grains additionally show homogeneous bright-CL response rims. Th/U ranges from 0.2 to 1.1 for the magmatically zone zircons and is < 0.1 for the bright-CL response rims.

From this sample 25 analyses were made, of which 23 plot on a discordia line with an upper intercept at 1162 ± 19 Ma and a lower intercept at 564 ± 47 Ma (Fig. 6c). The main population plots close to the upper intercept and can be refined using 18 analyses to give a weighted mean $^{207}Pb/^{206}Pb$ age of 1143 ± 11 Ma (MSWD = 1.0), or 14 analyses to give to an equivalent concordia age of 1141 ± 7 Ma (Fig. 6d). The weighted mean and concordia ages are interpreted to date the emplacement of this rock, the lower intercept is taken to date Pb-loss due to Pan-African metamorphism.

Sample **NY8671–2** is the southernmost sample, from a ~2 km long sheet-like intrusive body near the tectonic boundary between the Ufipa and Nyika subdomains. It is a mesocratic, granitic orthogneiss (locally with K-feldspar augen), with leucocratic veins forming a stockworks-type pattern. Zircons from this rock are subhedral to euhedral in habit and in CL images show concentric magmatic growth zoning that is partly replaced by areas of recrystallised zircon. Some zircons grains contain distinct cores. Th/U is between 0.1 and 1.8, whereas the three youngest grains have lower Th/U between 0.05 and 0.2.

Forty-four analyses were made from this sample with a significant proportion of the dataset yielding mildly to significantly discordant data

(Fig. 6e). Considering the data that are <15% discordant, individual $^{207}Pb/^{206}Pb$ show a near continuous spread of dates between ~1210 Ma and 950 Ma. These data are not straightforward to interpret; one possibility is to exclude the youngest three grains, which are distinct outliers (Fig. 6e), then split the remaining data into two arbitrary age groups of 13 and 14 analyses that yield quite low MSWD values for their combined ages. These age groups yield weighted mean $^{207}Pb/^{206}Pb$ ages of 1142 ± 6 Ma (MSWD = 1.2) and 1176 ± 7 Ma (MSWD = 1.9), respectively. The age groups can, additionally, be combined with a number of more discordant analyses (Fig. 6e) to produce discordia lines that project through the origin and produce upper intercept ages of 1148 ± 5 Ma (MSWD = 1.2) and 1190 ± 8 Ma (MSWD = 3.6). The remaining three outlying grains yield $^{207}Pb/^{206}Pb$ dates of 985 ± 10 Ma, 962 ± 13 Ma and 954 ± 11 Ma. The scatter in the dataset makes any conclusions drawn from these data somewhat uncertain. However, a reasonable interpretation is that the older age group (1176 ± 7 Ma) dates inherited xenocrysts present in this sample. The younger population (1142 ± 6 Ma) is then the best estimate for the timing of emplacement of the igneous protolith of this rock. The youngest three grains (~960 Ma), which plot separately (Fig. 6e) and have lower Th/U (<0.2), may represent evidence for a presently poorly constrained and documented post-Irumide event in northern Malawi. Equivalent ages are reported for aplitic and micro-granite dykes (Ring et al., 1999) and from a quartz syenite intrusion, which crops out further south in the Ubendian domain (Thomas et al., 2022a).

5.2.5. *Luromo granite*

The Luromo Granite (Ring et al., 1999; Charles et al., 2022) is a very small intrusion (<1 km^2) exposed in the Luromo Peninsula which projects into Lake Malawi, along with a number of offshore islands and rocks. It consists of foliated granite (quartz, oligoclase, microcline and biotite ± amphibole), and is associated with microgranite and aplite dykes. It contains many enclaves of biotite-bearing paragneiss derived from the Ubendian country rocks. The eastern part is feldspar megacrystic. This small body was dated by Ring et al. (1999) at 1108 ± 1 Ma and although no samples were taken as part of the current study, it is included here for completeness.

6. Whole-rock radiogenic isotope data

A dated sample from the Mwakikome orthogneiss and Mwenga Suite granites were analysed for Sm–Nd and Rb–Sr isotopes. The data are presented in supplementary Appendix 4. The Mwakikome orthogneiss (KA8350) has an ϵNd of −4.5 and a two-stage NdT_{DM} age of 2.27 Ga. Mwenga Suite sample NY8671-2) has an ϵNd of −2.2 and a two-stage NdT_{DM} age of 1.88 Ga. The two-stage model age calculations (after de Paolo et al., 1991) used the age of each sample as in Appendix 4, and a depleted mantle composition from Bea et al. (2023). $^{87}Sr/^{86}Sr$ is calculated at 550 Ma, the last major thermal event recognised in the Ubendian Domain. The Mwakikome orthogneiss has an $^{87}Sr/^{86}Sr_{(t)}$ of 0.7378 and the Mwenga Suite sample recorded 0.7928.

Both Nd and Sr isotopic values indicate that the Mwakikome orthogneiss and Mwenga Suite are evolved rocks that were melted, to a large degree, from sources extracted from the mantle in the Palaeoproterozoic. The strongly radiogenic $^{87}Sr/^{86}Sr_{(t)}$ recorded by both rocks suggest that these Palaeoproterozoic source rocks were unlikely to have been previously melted prior to the extraction of the partial melts that produced the Mwakikome and Mwenga granitoids. The new U–Pb zircon geochronology and radiogenic isotope data are summarised in Table 1.

7. Whole-rock major and trace element geochemistry

Nine samples of the Mwenga Suite granites were analysed for whole-rock major and trace element geochemistry (supplementary Appendix 5). This includes all the dated samples and two additional samples collected from the quarry in the Mwenga pluton, close to KA273. The major elements show a fairly narrow compositional range with SiO_2 between 69 and 77 wt%. K_2O (4.6–6.1 wt%) and Na_2O (2.0–3.5 wt%) are notably more abundant than CaO (0.5–1.9 wt%) as is Fe_T (1.8–5.6 wt %) when compared to MgO (<0.1–0.5 wt%), so the Mwenga Suite intrusions consequently classify as sub-alkaline granite with respect to SiO_2 versus alkalis ($Na_2O + K_2O < 9.5$) and ferroan with $Fe^* > 0.8$ (Fig. 7a and b). On a normative basis the Mwenga Suite classify as alkali-feldspar granite, syeno- and monzogranite (Fig. 7c). The less silicic rocks (syenogranites) are metaluminous (ASI<1.0), with a trend to more peraluminous (ASI>1.0) compositions with increasing SiO_2 (Fig. 7d).

The ranges of trace element concentrations are also rather restricted and consistent. Primitive mantle-normalised trends on a spider diagram for the Mwenga Suite are relatively smooth between Cs and Pr, although with a shallow negative Nb–Ta anomaly. The remainder of the elements show more fractionation and include deep negative Sr–P and Ti anomalies (Fig. 8a). Normalised HREE concentrations vary between approximately 6 and 12. Chondrite-normalised REE patterns show limited overall fractionation, characterised by a relatively low mean $(La/Lu)_N$ of 14 (Fig. 8b). Most fractionation occurs between the LREE and MREE, with mean $(La/Sm)_N = 5$ and mean $(Gd/Lu)_N = 1.6$. All samples show a distinctive negative Eu anomaly with a mean Eu/Eu* equal to 0.5.

On tectonic discrimination diagrams the samples from the Mwenga Suite exhibit within-plate and A-Type granite signatures (Fig. 9a and b). On the Nb + Y versus Rb and Nb versus Y plots of Pearce et al. (1984), there is some major element control on the observed data scatter. The syenogranite samples record the strongest within-plate signals on both plots, while the alkali feldspar granites and monzogranites plot closer to the volcanic-arc/collision granite boundary. One outlying sample (KA2701) plots within the volcanic arc field. The A-Type granite character of the majority of the rocks is mirrored in the Zr versus Ga/Al plot of Whalen et al. (1987). In this plot sample KA 2701 is again anomalous and shows a more I/S-type character (Fig. 9c). It is noteworthy that this sample also was the only rock to have a very large Palaeoproterozoic

Table 1
Summary of U–Pb zircon ages (in Ma) and radiogenic isotope data of the Mwenga Suite and Mwakikome Granite (KA8350), Ubendian Domain. (568 ± 12* = weighted mean Pb^{206}/U^{238} age of 4 metamorphic grains). US = University of Stellenbosch, BRGM = Bureau de Recherches Géologiques et Minières, GTK = Geological Survey of Finland.

Pluton	Sample number	Upper intercept age	Weighted mean $Pb^{207}/^{206}$ age	Concordia age	Inheritance age	Lower intercept age	**NdTdm (Ga)**	ϵNd	$^{87}Sr/^{86}Sr_{550}$	Analytical Laboratory
Mwenga	KA2723	1145 ± 19	1138 ± 12	1130 ± 5		~500				US
Lwakwa	KA8175-2	1162 ± 13	1136 ± 6	1128 ± 3	~1260	~550				BRGM
	KA19428-1	1129 ± 20	1139 ± 13	1143 ± 5	1224 ± 27	~500				GTK
Wililo	KA2638	1167 ± 28	1118 ± 15	1119 ± 6		547 ± 38, *568 ± 12**				US
	KA2701	1115 ± 22	1114 ± 20	1118 ± 8	~2000, 2500	0				US
Minor southern	NY6545	1162 ± 19	1143 ± 11	1141 ± 7		562 ± 47				US
intrusions	NY8671-2	1148 ± 5	1142 ± 6		~1175	0	1.88	−2.2	0.79283	BRGM
Mwakikome	KA8350	1417 ± 3	1411 ± 3	1417 ± 3		0	2.27	−4.5	0.7378	BRGM

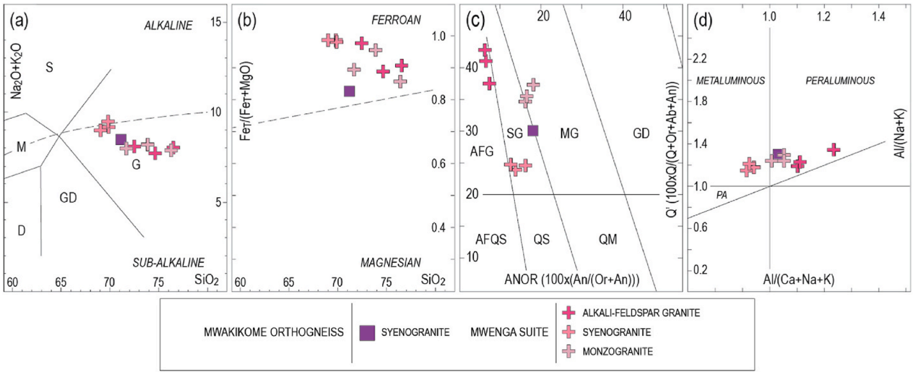

Fig. 7. Major element composition plots of the Mwenga Suite. a) Silica versus alkalis (after Cox et al., 1979); b) silica versus Fe* (=FeT/FeT + MgO), after (Frost and Frost, 2008); c) normative ANOR versus Q′ plot of Streckeisen and Le Maitre (1979); d) "Shand Index" of Maniar and Piccoli (1989). Abbreviated field names are: AFG = Alkali-feldspar granite, AFQS = Alkali-feldspar quartz syenite, D = diorite, G = granite, GD = Granodiorite, M = Monzonite, MG = monzogranite, PA=Peralkaline, QM = Quartz monzonite, QS = Quartz syenite.

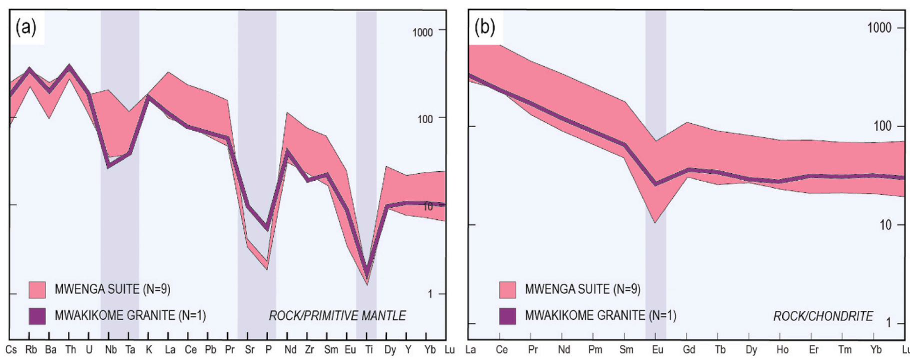

Fig. 8. Trace element composition plots for the Mwenga Suite and the Mwakikome orthogneiss. a) Selected trace elements normalised to primitive mantle, b) Rare earth elements normalised to Chondrite. Normalisation values for both plots are from Sun and McDonough (1989).

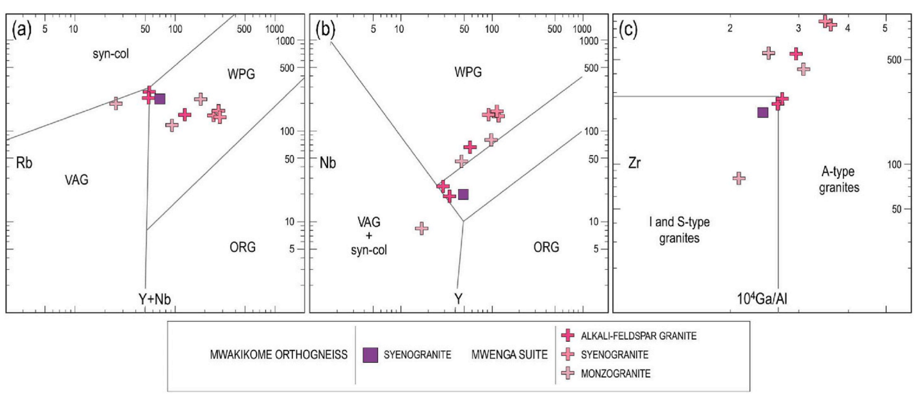

Fig. 9. Tectonic environment discrimination plots of the Mwenga Suite and Mwakikome orthogneiss. a) and b) after Pearce et al. (1984), c) after Whalen et al. (1987). Abbreviated field names are: ORG=Ocean ridge granite, syn-col = syn-collisional granite, VAG = volcanic arc granite, WPG = within plate granite.

zircon population, showing a higher degree of country-rock contamination than the other samples.

The Mwakikome orthogneiss is a silicic intrusion with ~71 wt% SiO_2 and has $K_2O > Na_2O > CaO$ (5.3 wt%, 3.3 wt% and 1.5 wt% respectively). Total alkalis sum to ~8.5% and, similar to the rocks of the Mwenga Suite, the Mwakikome orthogneiss is sub-alkaline (Fig. 7a). ASI and Fe* equal 1.05 and 0.83 respectively, indicating that this intrusion is both ferroan and peraluminous (Fig. 7b, d). On a normative basis the Mwakikome orthogneiss classifies as a syenogranite (Fig. 7c). The primitive mantle-normalised trace element pattern for this sample is characterised by a relatively shallow negative Nb–Ta anomaly and deeper negative anomalies for Sr–P and Ti (Fig. 8). Normalised HREE concentrations are ~10. The chondrite-normalised REE pattern shows moderate enrichment of HREE relative to MREE, a shallow negative Eu anomaly (Eu/Eu* = 0.5) and little fractionation between MREE and HREE ($La/Sm_N = 5$ and $Gd/Lu_N = 1.2$). The fractionation between LREE and HREE, measured by $(La/Lu)_N$, is 11. When plotted on the Y + Nb versus Rb discrimination plot (Pearce et al., 1984), the Mwakikome orthogneiss plots in the within-plate field, but transitional between A-Type and I/S-Type on the Whalen et al. (1987) plot (Fig. 9).

8. Discussion

One of the enduring problems in the deciphering of polymetamorphic belts is the degree to which event (often themselves polyphase) are present and to what extent each phase has influenced the present-day configuration of the geology. The Mesoproterozoic granitic rocks described here form a valuable time marker between the two major crust-forming and orogenic episodes of NW Malawi, adjacent SW Tanzania and NE Zambia; the Ubendian (2.1-1.8 Ga) and Irumide (1.1-1.0 Ga) events. The 1411 ± 3 Ma Mwakikome Orthogneiss is a peraluminous and ferroan syenogranite (Fig. 7) that has a within-plate geochemical signature characterised by relatively high abundances of Nb–Ta and HREE and deep negative primitive mantle normalised anomalies for Sr–P and Ti (Fig. 8). Nearby coeval rocks include the Chimala Granite (1408 ± 6 Ma; Thomas et al., 2019), which intrudes the Ubendian "Upangwa terrane" of SW Tanzania and a slightly older orthogneiss (1435 ± 15 Ma; Thomas et al., 2016), that crops out in the Livingstone Mountains of SW Tanzania (Fig. 10).

This small, isolated cluster of ~1400 Ma intrusions is similar in age to the earliest "Kibaran" intrusive rocks from the Karagwe-Ankole belt of central Africa, situated >700 km NW of Malawi. These are shown on Fig. 10, which is a time-slice map of East Africa at ~1100 Ma, prior to the Irumide orogeny (with some younger cover rocks shown which obscure the older geology). These early "Kibaran" rocks are comprised of differentiated mafic–ultramafic intrusions (Maier et al., 2007; Zi et al., 2019) that pre-date, by at least ~10 Ma, the onset of the main phase of voluminous, widely-distributed Kibaran magmatism between ~1390 and 1330 Ma (Kokonyangi et al., 2004; Buchwaldt et al., 2008; Tack et al., 2010; Mäkitie et al., 2014; Nambaje et al., 2021). This igneous activity was bimodal and produced mafic rocks that intruded either as an arcuate dyke swarm into Ubendian-age basement rocks

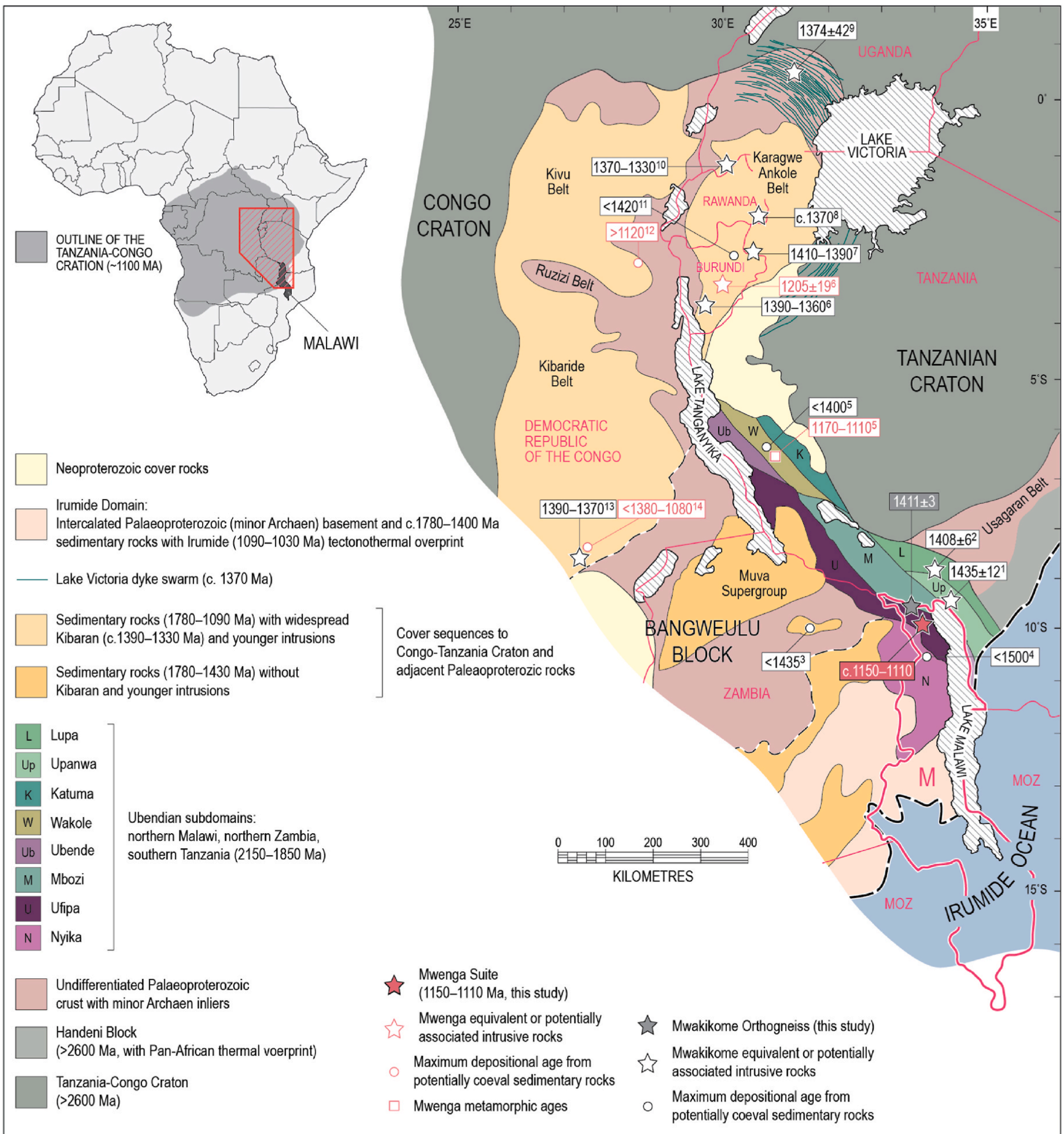

Fig. 10. Geological map of Precambrian geology of central East Africa at ~1100 Ma. Inset upper left: Location of the Tanzania-Congo Craton in Africa. Red box outlines the region enlarged on the right. Main image: Geology of the SE part of the Tanzania-Congo Craton illustrating the distribution of rocks with Mwakikome-like (black text, white background) and Mwenga-like (red text, white background) ages. Abbreviated country names: M = Malawi, Moz = Mozambique. Superscripts give sources of data: [1] Thomas et al. (2019), [2] Thomas et al. (2016), [3] De Waele and Fitzsimons (2007), [4] Thomas et al. (2022b), [5] Boniface et al. (2014), [6] Tack et al. (2010), [7] Maier et al. (2007), [8] Nambaje et al. (2021), [9] Mäkitie et al. (2014), [10] Buchwaldt et al. (2008), [11] Fernandez-Alonso et al. (2012), [12] Villeneuve et al. (2019), [13] Kokonyangi et al. (2004) and [14] Kokonyangi et al. (2007).

(Fig. 10) or as layered mafic to ultramafic sills into late Palaeoproterozoic and Mesoproterozoic sedimentary cover rocks (Duchesne et al., 2004; Maier et al., 2008; Mäkitie et al., 2014). The voluminous coeval silicic intrusions are comprised mostly of peraluminous and sub-alkaline monzogranite and syenogranite (Kokonyangi et al., 2004; Buchwaldt et al., 2008; Debruyne et al., 2015; Nambaje et al., 2021) that are compositionally very similar to the Mwakikome orthogneiss.

The bimodal nature of Kibaran igneous activity together with the chemistry of both mafic and felsic intrusions is widely, but not exclusively, interpreted to suggest that they were emplaced during a long-lived period of extension and intra-cratonic basin formation from ~1780 Ma to ~1380 Ma (Tack et al., 2010; Fernandez-Alonso et al., 2012). One such episode of extension and coeval sediment deposition began around 1420 Ma and continued until at least ~1370 Ma (Fernandez-Alonso et al., 2012; Koegelenberg et al., 2015). During this interval Kibaran igneous rocks intruded as sill and plutons within the existing sedimentary pile and occurred as surface flows of basalt and effusive felsic tuffs on the basin floor (Fernandez-Alonso et al., 2012). In northern Malawi, there are a variety of small mafic bodies within the Ubendian gneisses (Fullgraf et al., 2021), but none of these has been dated. The degree to which Mwakikome magmatism in northern Malawi was also bimodal cannot currently be answered.

Nevertheless, the striking compositional similarities between the silicic Kibaran-age intrusions shown on Fig. 10 and the Mwakikome orthogneiss suggest both groups of rocks likely formed in a similar tectonic setting. By comparison with central Africa, where evidence for coeval magmatism and sedimentation is well preserved, a definitive coeval sedimentary record is lacking in Malawi. It is, however, hinted at by a number of nearby exposures of post-Ubendian sedimentary rocks that yield maximum depositional ages close to the onset of Mwakikome igneous activity. These include: (1) A fault-bound layer of Mafingi Group schist exposed in the Nyika Subdomain of northern Malawi (maximum depositional age = ~1500 Ma; Thomas et al., 2022b), (2) the Kasama Formation of NE Zambia (maximum depositional age = ~1430 Ma; De Waele and Fitzsimons, 2007) and, (3) the argillitic metasedimentary rocks of the Ubendian Wakole Subdomain with maximum depositional ages of ~1400 Ma (Boniface et al., 2014). The geographic distribution of these rocks is illustrated in Fig. 10.

The ~1150–1110 Ma granitoids of the Mwenga Suite are compositionally very similar to the Mwakikome orthogneiss. They comprise weakly metaluminous-peraluminous, sub-alkaline and ferroan alkali-feldspar granite, syenogranite and monzogranite (Fig. 7). The trace element compositions of the Mwenga and Mwakikome orthogneiss are similar (Fig. 8), although the former tend to have higher concentrations of Nb, Ta, Y, Zr, Ga/Al and HREE and thus yield stronger within-plate signatures (Fig. 9). Nd isotopic data from a Mwenga Suite intrusion (ϵNd = −2.2, NdTDM = 1.88 Ga) imply that these rocks are evolved, and partially sourced from their Ubendian host rocks, although with an important mantle component. This inference, together with the compositional similarity observed for the Mwenga and Mwakikome rocks, suggest both phases of magmatism occurred in similar extensional tectonic settings. It is important to note that the Mwenga Suite is considerably older than the granitoid orthogneisses of the adjacent Irumide belt in Malawi, which give ^{207}Pb/^{206} Pb weighted mean ages ranging from ~1060 to 1030 Ma (Thomas et al., 2022c) and ~1050 to 950 Ma in Zambia (see review of De Waele et al., 2006). The intrusions of the Mwenga Suite consequently pre-dates the granitoids within the Irumide belt and lie ~150 km inboard of the Irumide orogenic front. Although the Mwenga Suite intrusions are comparatively small, they form an important component of the Ufipa Subdomain in northern Malawi (Fig. 1). It is consequently surprising that coeval granitoids have not been reported from other areas of central and southern Africa (Fig. 10). There are zircon and monazite ages of ~1170–1110 Ma from garnet-kyanite schists from the Wakole Subdomain in Tanzania (Fig. 10), but these are interpreted to date moderate pressure, middle-to upper amphibolite facies metamorphism (Boniface et al. (2014), which seems at odds with the extension tectonic setting implied by the Mwenga Suite.

From the southern Karagwe-Ankole Belt Tack et al. (1994, 2010) describe the 40 km long "Gitega-Makebuko-Bukirasazi alignment" in Rwanda-Burundi (Location with superscript "6" in Fig. 10) comprised predominantly of ~1205 Ma A-type granitoids, syenites, and associated subordinate mafic rocks. While these rocks predate the Mwenga Suite by some 70 Myr, they are geochemically comparable. The more silicic Gitega-Makebuko-Bukirasazi granitoids are sub-alkaline to weakly alkaline ferroan alkali-feldspar granites, syenogranites and monzogranites that plot well within the within-plate and A-type granites fields of Pearce et al. (1984) and Whalen et al. (1987). This potentially indicates that a wide area of central-eastern Africa experienced geographically dispersed and diachronous pulses of intra-plate magmatism in the period between ~1400 and 1100 Ma.

Support for the generation and emplacement of the granitoids of this period in an extensional geodynamic setting is given by presence of coeval sedimentary rocks. For example, components of the Bugarama and Nya-Ngezie groups in the Kivu-Maniema area of the Democratic Republic of the Congo (Fig. 10) have yielded maximum depositional ages of ~1210 Ma and 1120 Ma respectively (Villeneuve et al., 2019). From the Kibaride Belt to the south, Kokonyangi et al. (2007) constrained the deposition of the Nzilo Group to between 1380 Ma and 1080 Ma, also allowing deposition in the 1210–1110 Ma intervals of A-type magmatism in the Karagwe-Ankole Belt (Tack et al., 2010) and northern Malawi (this study). Equivalent sedimentary rocks are not recorded from areas further to the east, although it is noteworthy that a number of whole rock Rb–Sr ages from the Karagwe-Ankole Belt scatter between ~1260 and 1110 Ma (Lavreau and Liégeois, 1982; Klerkx et al., 1984, 1987; Tack et al., 1990, 1994). These ages were originally interpreted to date granite emplacement, although subsequent U–Pb zircon studies have shown that the Rb–Sr ages are considerably younger than the intrusive ages (Tack et al., 2010). It might thus be that the Rb–Sr ages reflect thermal resetting associated with a combination of burial beneath a thick sedimentary cover and a rising geothermal gradient associated with crustal thinning and, possibly, magmatic underplating.

Both the Mwenga Suite and the Mwakikome orthogneiss intruded close to the margin of the Archaean Tanzania Craton, as do the majority of the broadly Kibaran igneous rocks exposed further to the NW. In addition, most of the Mesoproterozoic sedimentary cover rocks in the region overlie Ubendian-age Palaeoproterozoic crust flanking the craton margin (Fig. 10). If, as we contend, these igneous and sedimentary rocks reflect a long-lived period of intra-cratonic extension and basin formation, it is tempting to suggest that the localisation of both the igneous rocks and the concomitant sedimentary rocks along the craton margin reflects a long-lived line of inherent weakness that was repeatedly reactivated during the Mesoproterozoic.

Allied to the above discussion, the Mwenga Suite and the Mwakikome orthogneiss show a strong and consistent NW-SE (Ubendian trend) penetrative ductile foliation that is broadly parallel to the SW margin of the Tanzania Craton (Fig. 10). This suggests that the margin was again reactivated, most likely during the late Ediacaran, as a distal effect of the Pan-African orogeny. This conclusion was reached by Ring et al. (1999) and is supported by the Pb-loss discordia lines recorded in five of the seven dated samples presented here that project toward a ~550 Ma lower intercept. K–Ar biotite and hornblende ages from Mwenga granitoids also yield ages between 590 and 530 Ma (Ray, 1974; Ring et al., 1999). It is thus relevant that the Mwenga Suite and the Mwakikome orthogneiss are spatially associated with, and deformed by, mylonites that form an anastomosing network of schist belts and shear zones in northern Malawi (Fig. 1). Collectively these structures define the Pan-African Mugesse Shear Zone, which preserves sinistral strike-slip kinematics and developed under greenschist-facies to amphibolite metamorphic conditions (Ring et al., 1999). The discrete nature of the shearing implies that the Ubendian Domain was little affected by the effects of the Irumide orogeny and supports the contention of Fitches

(1971) that effects of the Irumide orogenyare unimportant east of the Mafingi Hills.

9. Conclusions

The Mwakikome orthogneiss is a small pluton of ~1400 Ma syenogranite and one of a small number of such intrusions in northern Malawi and SW Tanzania. These rocks possibly represent the earliest phase Kibaran-aged (c. 1390–1330 Ma) intra-plate magmatism that is more voluminously developed in the Karagwe-Ankole, Kivu and Kibaride Belts several hundred kilometres to the west and NW.

The Mwenga Suite comprises a number of NW-SE trending and elongated alkali-feldspar granite, syenogranite and monzogranite orthogneisses that form sheet-like plutons and associated minor intrusions emplaced between ~1150 and 1110 Ma. They are restricted to the Ufipa Subdomain of the Ubendian Domain, most especially in its core, which may indicate re-activated zones of Ubendian-age crustal weakness. The rocks presently have no reported temporal correlates and appear to be unique to northern Malawi (Fig. 10).

Both the Mwakikome and Mwenga rocks do, however, build on a theme of punctuated periods of intra-plate extension, basin formation, and bimodal A-type magmatism in central and eastern Africa during the Mesoproterozoic (Tack et al., 2010; Fernandez-Alonso et al., 2012). These events pre-date, and were potentially terminated by, convergent Irumide orogenesis between 1090 and 1030 Ma that is widely developed in central and southern Malawi and southern Zambia (Johnson et al., 2005), and whose distal effects are interpreted to have folded the strata of the Karagwe-Ankole, Kivu and Kibaride Belts (Kokonyangi et al., 2004; Fernandez-Alonso et al., 2012).

The Irumide orogenesis does not appear to have affected the rocks of the Ubendian Domain of northern Malawi and the observed fabrics in Mwakikome and Mwenga intrusions were imposed during Pan-African transcurrent tectonics associated with the Mugesse set of shear zones.

Declaration of competing interest

The authors declare that they have no known competing financial interests or personal relationships that could have appeared to influence the work reported in this paper.

Data availability

data is in supplemementary files

Acknowledgements

The authors thank careful reviews of the manuscript by Steve McCourt and Andreas Möller which led to considerable improvement of the paper.

Appendix A. Supplementary data

Supplementary data to this article can be found online at https://doi.org/10.1016/j.jafrearsci.2023.104897.

References

Bea, F., Montero, P., Barcos, L., Cambeses, A., Molina, J.F., Morales, I., 2023. Understanding Nd model ages of granite rocks: the effects of the ^{147}Sm/^{144}Nd variability during partial melting and crystallization. Lithos 436–437, 106940. https://doi.org/10.1016/j.lithos.2022.106940.

Boniface, N., Schenk, V., Appel, P., 2014. Mesoproterozoic high-grade metamorphism in pelitic rocks of the northwestern Ubendian Belt: implication for the extension of the Kibaran intra-continental basins to Tanzania. Precambrian Res. 249, 215–228.

Buchwaldt, R., Toulkeridis, T., Todt, W., Ucakuwun, E.K., 2008. Crustal age domains in the Kibaran belt of SW-Uganda: combined zircon geochronology and Sm–Nd isotopic investigation. J. Afr. Earth Sci. 51, 4–20.

Charles, N., Callec, Y., Bailly, L., Fullgraf, T., Thomas, R.J., Boger, S.D., Hyvönen, E., Zammit, C., Dombola, K., 2022. Uzumara North 41N, 1:100 000 Geological Map Series, Sheet Explanation. Geological Survey Department, Zomba, Malawi, p. 60.

Cox, K.G., Bell, J.D., Pankhurst, R.J., 1979. The Interpretation of Igneous Rocks. George Allen and Unwin.

Daly, M.C., 1988. Crustal shear zones in central Africa: a kinematic approach to Proterozoic tectonics. Episodes 11, 5–11.

Debruyne, D., Hulsbosch, N., Van Wilderode, J., Balcaen, L., Vanhaecke, F., Muchez, P., 2015. Regional geodynamic context for the Mesoproterozoic Kibara Belt(KIB) and the Karagwe-Ankole Belt: Evidence from geochemistry andisotopes in the KIB. Precam. Res. 264, 82–97. https://doi.org/10.1016/j.precamres.2015.04.001.

DePaolo, D.J., Linn, A.M., Schubert, G., 1991. The continental crustal age distribution: methods of determining mantle separation ages arom Sm-Nd isotopic data and application to the Southwestern United States. J. Geophys. Res. 96 (B2), 2071–2088.

De Waele, B., Kampunzu, A.B., Mapani, B.S.E., Tembo, F., 2006. The mesoproterozoic Irumide belt of Zambia. J. Afr. Earth Sci. 46, 36–70. https://doi.org/10.1016/j.jafrearsci.2006.01.018.

De Waele, B., Fitzsimons, I.C.W., 2007. The nature and timing of Palaeoproterozoic sedimentation at the southeastern margin of the Congo Craton; zircon U–Pb geochronology of plutonic, volcanic and clastic units in northern Zambia. Precambrian Res. 159, 95–116.

Duchesne, J.-C., Liégeois, J.-P., Deblond, A., Tack, L., 2004. Petrogenesis of the Kabanga–Musongati layered mafic–ultramafic intrusions in Burundi (Kibaran Belt): geochemical, Sr–Nd isotopic constraints and Cr–Ni behaviour. J. Afr. Earth Sci. 39, 133–145.

Fernandez-Alonso, M., Cutten, H., DeWaele, B., Tack, L., Tahon, A., Baudet, D., Barritt, S. D., 2012. The Mesoproterozoic Karagwe-Ankole Belt (formerly the NE Kibara Belt): the result of prolonged extensional intracratonic basin development punctuated by two short-lived far-field compressional events. Precambrian Res. 216–219, 63–86.

Fitches, W.R., 1971. Sedimentation and tectonics at the northeast end of the Irumide orogenic belt, N. Malawi and Zambia. Geol. Rundsch. 60 (2), 589–619.

Fitches, W.R., Ray, G.E., 1980. Geological Map of the Chitipa Area at 1: 100 000 Scale. Malawi Government, 1 sheet.

Frost, B.R., Frost, C.D., 2008. A geochemical classification for feldspathic igneous rocks. J. Petrol. 49, 1955–1969.

Fullgraf, T., Thomas, R.J., Boger, S.D., Callec, Y., 2021. Geological Map of Malawi at 1: 1 000 000 (With Notes). Geological Survey Department, Zomba, Malawi.

Johnson, S.P., Rivers, T., De Waele, B., 2005. A review of the Mesoproterozoic to early Palaeozoic magmatic and tectonothermal history of south–central Africa: implications for Rodinia and Gondwana. J. Geol. Soc. London 162, 433–450.

Klerkx, J., Liégeois, J.P., Lavreau, J., Theunissen, K., 1984. GranitoÏdes kibariens précoces et tectonique tangentielle au Burundi: magmatisme bimodal lié à une distension crustale. In: Klerkx, J., Michot, J. (Eds.), African Geology, a Volume in Honour of L. Cahen. Royal Museum for Central Africa, Tervuren, pp. 29–46.

Klerkx, J., Liégeois, J.-P., Lavreau, J., Claessens, W., 1987. Crustal evolution of the northern kibaran belt, eastern central Africa. In: Kröner, A. (Ed.), Proterozoic Lithospheric Evolution. American Geophysical Union Geodynamics Series, vol. 17, pp. 217–233.

Koegelenberg, C., Kisters, A.F.M., Kramers, J.D., Frei, D., 2015. U–Pb detrital zircon and39Ar–40Ar muscovite ages from the easternparts of the Karagwe-Ankole Belt: tracking Paleoproterozoic basin formation and Mesoproterozoic crustal amalgamation along the western margin of the Tanzania Craton. Precambrian Res. 269, 147–161.

Kokonyangi, J., Armstrong, R., Kampunzu, A.B., Yoshida, M., Okudaira, T., 2004. U–Pb zircon geochronology and petrology of granitoids from Mitwaba (Katanga, Congo): implications for the evolution of the Mesoproterozoic Kibaran belt. Precambrian Res. 132, 79–106.

Kokonyangi, J.W., Kampunzu, A.B., Armstrong, R., Arima, M., Yoshida, M., Okudaira, T., 2007. U-Pb SHRIMP dating of detrital zircons from the Nzilo group (kibaran belt): implications for the source of sediments and mesoproterozoic evolution of central Africa. J. Geol. 115, 99–113.

Lavreau, J., Liégeois, J.P., 1982. Granites à étain et granito-gneiss burundiens au Rwanda (région de Kibuye): âge et signification. Ann. Soc. Géol. Belgique 105, 289–294.

Le Bayon, B., Bailly, L., Thomas, R.J., Fullgraf, T., Boger, S.D., Hyvönen, E., Zammit, C., Dombola, K., 2022. Chitipa 42W, 1:100 000 Geological Map Series, Sheet Explanation. Geological Survey Department, Zomba, Malawi, p. 60.

Maier, W.D., Barnes, S.-J., Bandysyera, D., Livesey, T., Li, C., Ripley, E., 2008. Early Kibaran rift-related mafic–ultramafic magmatism in western Tanzania and Burundi: petrogenesis and ore potential of the Kapalagulu and Musongati layered intrusions. Lithos 101, 24–53.

Maier, W.D., Peltonen, P., Livesey, T.T., 2007. The ages of the Kabanga North and Kapalagulu intrusions, western Tanzania: a reconnaissance study. Econ. Geol. 102, 147–154.

Mäkitie, H., Data, G., Isabirye, E., Mänttäri, I., Huhma, H., Klausen, M.B., Pakkanen, L., Virransalo, P., 2014. Petrology, geochronology and emplacement model of the giant 1.37 Ga arcuate Lake Victoria Dyke Swarm on the margin of a large igneous province in eastern Africa. J. Afr. Earth Sci. 97, 273–296.

Maniar, P.D., Piccoli, P.M., 1989. Tectonic discrimination of granitoids. Geol. Soc. Am. Bull. 101, 635–643. https://doi.org/10.1130/0016-7606.

Nambaje, C., Satish-Kumar, M., Williams, I.S., Takahashi, T., Sajeev, K., 2021. Granitic rocks from Rwanda: vital clues to the tectonic evolution of the karagwe–ankole belt. Lithos 404–405, 106490.

Pearce, J.A., Harris, N.B.W., Tindle, A.G., 1984. Trace element discrimination diagrams for the tectonic interpretation of granitic rocks. J. Petrol. 25, 956–983.

Ray, G.E., 1974. The structural and metamorphic geology of northern Malawi. J. Geol. Soc. London 130, 427–440.

Ray, G.E., 1975. The geology of the Chitipa-Karonga area. Geological Survey Department, Bulletin 42, 101.

Ring, U., 1993. Aspects of kinematic history and mechanisms of superposition of the Proterozoic mobile belts of eastern Central Africa (northern Malawi and southern Tanzania). Precambrian Res. 62, 207–226.

Ring, U., Kröner, A., Layer, P., Buchwaldt, R., Toulkeridis, T., 1999. Deformed A-type granites in northern Malawi, east-central Africa: pre- or syntectonic? J. Geol. Soc. London 156, 695–714.

Stephens, E.A., Ray, G.E., 1978. Geological Map of the Karonga Area, Malawi. Geological Survey Department, Zomba, Malawi.

Stephens, E.A., Ray, G.E., Fitches, W.R., 1991. Geological Map of the Karonga Area (With Notes). Geological Atlas of Malawi. Sheet 10, 1: 250 000 series geological map, first ed. Geological Survey Department, Zomba, Malawi.

Streckeisen, A.L., Le Maitre, R.W., 1979. A chemical approximation to the modal QAPF classification of the igneous rocks. Neues Jahrbuch fur Mineralogie, Abhandlungen 136, 169–206.

Sun, S.S., McDonough, W.F., 1989. Chemical and isotopic systematics of ocean basalts: implications for mantle composition and processes. In: Saunders, A.D., Norry, M.J. (Eds.), Magmatism in Ocean Basins, vol. 42. Geol. Soc. London, Special Publications, pp. 313–345.

Tack, L., De Paepe, P., Liégeois, J.P., Nimpagaritse, G., Ntungicimaye, A., Midende, G., 1990. Late kibaran magmatism in Burundi. J. Afr. Earth Sci. 10, 733–738.

Tack, L., Liégeois, J.P., Deblond, A., Duchesne, J.C., 1994. Kibaran A-type granitoids and mafic rocks generated by two mantle sources in a late orogenic setting (Burundi). Precambrian Res. 68, 323–356.

Tack, L., Wingate, M.T.D., De Waele, B., Meert, J., Belousova, E., Griffin, W., Tahon, A., Fernandez-Alonso, M., 2010. The 1375 Ma "Kibaran Event" in Central Africa: prominent emplacement of bimodal magmatism under extensional regime. Precambrian Res. 180, 63–84. https://doi.org/10.1016/j.precamres.2010.02.022.

Thomas, R.J., Spencer, C., Bushi, A.M., Baglow, N., Boniface, N., de Kock, G.S., Horstwood, M.S.A., Hollick, L., Jacobs, J., Kajara, S., Kamihanda, G., Key, R.M., Maganga, Z., Mbawala, F., McCourt, W.J., Momburi, P., Moses, F., Mruma, A., Myambilwa, Y., Roberts, N.M.W., Saidi, H., Nyanda, P., Nyoka, K., Millar, I., 2016. Geochronology of the central Tanzania Craton and its southern and eastern orogenic margins. Precambrian Res. 277, 47–67. https://doi.org/10.1016/j.precamres.2016.02.008.

Thomas, R.J., Jacobs, J., Mruma, A., Elburg, M., Kamihanda, G., Kankila, A., Masanja, A., Saidi, H., 2019. New U-Pb-Hf zircon isotope data for the Paleoproterozoic Ubendian belt in the Chimala area, SW Tanzania. Geosci. Front. 10, 1003–2006. https://doi.org/10.1016/j.gsf.2018.05.010.

Thomas, R.J., Callec, Y., Bailly, L., Fullgraf, T., Boger, S.D., Hyvönen, E., Zammit, C., Dombola, K., 2022a. Karonga 42E, 1:100 000 Geological Map Series, Sheet Explanation. Geological Survey Department, Zomba, Malawi, p. 98.

Thomas, R.J., Fullgraf, T., Nicolas, C., Le Bayon, B., Boger, S.D., Frei, D., Lach, P., Dombola, K., 2022b. Age and correlation of the proterozoic Mafingi group in Malawi. J. Afr. Earth Sci. https://doi.org/10.1016/j.jafrearsci.2022.104723.

Thomas, R.J., Boger, S.D., Fullgraf, T., Bracciali, L., Frei, D., Le Roux, P., Lach, P., Lahay, Y., Ruffet, G., 2022c. Geochronology and Radiogenic Isotopes (U-Pb Single Zircon, Sm-Nd Whole Rock, Ar-Ar Muscovite). GEMMAP Memoir Series #2. Geological Survey Department, Zomba, Malawi, p. 116, 3 appendices.

Villeneuve, M., Gärtner, A., Kalikone, C., Wazi, N., Hofmann, M., Linnemann, U., 2019. U-Pb ages and provenance of detrital zircon from metasedimentary rocks of the Nya-Ngezie and Bugarama groups (D.R. Congo): a key for the evolution of the Mesoproterozoic Kibaran-Burundian Orogen in Central Africa. Precambrian Res. 328, 81–98.

Whalen, J.B., Currie, K.L., Chappell, B.W., 1987. A-type granites: geochemical characteristics, discrimination and petrogenesis. Contrib. Mineral. Petrol. 95, 407–419.

Zi, J.-W., Rasmussen, B., Muhling, J.R., Maier, W.D., Fletcher, I.R., 2019. U-Pb monazite ages of the Kabanga mafic-ultramafic intrusions and contact aureoles, central Africa: geochronological and tectonic implications. GSA Bulletin 131, 1857–1870.